Phase-rotated MR spectroscopy using dual-PRESS: theory and application in human brain

Saadallah Ramadan, M. Albert Thomas, and Carolyn E. Mountford

Citation: AIP Conference Proceedings **953**, 277 (2007); doi: 10.1063/1.2817350

View online: https://doi.org/10.1063/1.2817350

View Table of Contents: http://aip.scitation.org/toc/apc/953/1

Published by the American Institute of Physics

Phase-rotated MR spectroscopy using dual-PRESS: theory and application in human brain

Saadallah Ramadan[*,¥], M Albert Thomas[†] and Carolyn E Mountford [*,¥]

[*] *Department of Radiology, Brigham & Women's Hospital, Harvard Medical School, 75 Francis St Boston MA 02215, USA*
[†] *Radiology and Psychiatry, David Geffen School of Medicine at UCLA, Los Angeles, CA 90095, USA.*
[¥] *Previous Address: Institute for Magnetic Resonance Research University of Sydney NSW 2065 Australia*

Abstract. Phase-rotation spectroscopic acquisition is inherently different from the popular signal-averaging method. Phase-rotation will be described theoretically and experimentally in this article. Traditionally, a single echo is acquired in a PRESS or STEAM sequence at a particular TE. If a long-TE spectrum is desired, then another echo is usually acquired at a longer echo time. We here propose a method by which a pair of echoes, at short-TE and a long-TE, are acquired in one experiment, thus saving 50% of total acquisition time without significant sacrifice of spectral quality. The phase-rotation approach has been implemented with the proposed method. An additional benefit of the proposed Dual-PRESS method, is that it gives an insight into the transverse relaxation time constant, T2, for the various metabolites. The Dual-PRESS method is applied in phantom and in-vivo.

Keywords: Magnetic Resonance, Spectroscopy, phase-rotation, Dual-PRESS, T2 relaxation
PACS: 87.80.Lg, 87.85.-d, 87.55.kh

1. INTRODUCTION

Traditionally, one-dimensional (1D) magnetic resonance (MR) spectra are acquired using phase-cycling [1-3], where desired signals add coherently and unwanted signal add destructively. This selective constructive/destructive addition is implemented by carefully cycling the phases of the radio-frequency (RF) pulses and receiver (Rec) to particular values. Phase-rotation is an alternative approach by which signals from various coherences can be sorted out in a two-dimensional (2D) Fourier transformed (FT) map based on their unique phase characteristics. To date, the application of phase-rotation has been implemented in stimulated echo spectroscopy (STEAM) [4], point resolved spectroscopy (PRESS) [5] and double quantum localised spectroscopy [6]. In this article, a phase-rotation based acquisition will be described, both theoretically and experimentally, and its application in acquiring two echoes (Dual PRESS) in a single experiment will be introduced.

Hennig [5] was the first to propose a new method to acquire localised spectroscopic data, where by various scans are stored as rows in a two-dimensional (2D) matrix, which is then doubly Fourier transformed (FT) and a specific row is extracted to represent the 1D spectrum. A prime motivation of this new data acquisition/processing was to record MR spectra using a short echo time (TE) [4, 7-12]. Short TE-based sequences minimize signal loss due to T_2

CP953, *Data Mining, Systems Analysis, and Optimization in Biomedicine*
edited by O. Seref, O. E. Kundakcioglu, P. M. Pardalos

relaxation and reduce signal cancellation due to *J*-modulation, especially for short-T_2^* metabolites. However, TE in localised MR spectroscopy pulse sequences using phase-cycling schemes has to be long enough to allow time for the 'spoiler' or 'crusher' gradients to be applied, since the signals will be co-added in the end. In the phase-rotation method, however, spoilers are still needed but to a lesser extent since the undesired signal can be separated from the resonances of interest. Additionally, the demand on spoiler gradients to reduce unwanted signal increases in inhomogeneous magnetic or RF field [13]. Importantly, long TE-based acquisitions amplify motion artefacts and spoiling gradients also increase sensitivity to motion [14].

The minimum number of RF pulses in a localised pulse sequence is three, due to the requirement for localisation by three orthogonal slices where the intersection constitutes the region of interest or volume of interest (ROI/VOI). The number of single quantum signals occurring after the last RF pulse in a pulse sequence containing n RF pulses is $(3^{n-1}-1)/2$. A list of existing signals with their coherence transfer pathways (CTPs) [15] is shown in Table 1 gives the reader an insight into what signals need to be eliminated to obtain an uncontaminated spectrum.

TABLE 1. Types of existing signals in a three-pulse localisation sequence and their corresponding phase equations. Echo 12, 13 and 23 are obtained from two RF pulses only. STEAM N and STEAM P are stimulated echo and anti-echo signals [36], respectively.

Signal	Phase equation	CTP
FID 1	$\phi1$	−1,−1,−1
FID 2	$\phi2$	0,−1,−1
FID 3	$\phi3$	0,0,−1
Echo 12	$2\phi2-\phi1$	+1,−1,−1
Echo 13	$2\phi3-\phi1$	+1,+1,−1
Echo 23	$2\phi3-\phi2$	0,+1,−1
STEAM N	$\phi3+\phi2-\phi1$	+1,0,−1
STEAM P	$\phi3-\phi2+\phi1$	−1,0,−1
PRESS	$2\phi3-2\phi2+\phi1$	−1,+1,−1
DQF 1	$3\phi2-\phi1-\phi3$	+1,−2,−1
DQF 2	$3\phi3-\phi1-\phi2$	+1,+2,−1
DQF 3	$\phi1+\phi2-\phi3$	−1,−2,−1
DQF 4	$\phi1+3\phi3-3\phi2$	−1,+2,−1

In phase-rotation, each transient during, say a 128-average experiment, is acquired with a slightly different RF phase and saved as a row in a two-dimensional (2D) matrix, and the resulting time-phase matrix is then Fourier Transformed (FT) in both dimensions, then each signal in Table 1 will be shifted in the phase dimension by an amount proportional to the size of phase increment during the 128-average experiment and the phase equation in TABLE 1. Fourier Shift Theorem [16, 17] is the basis of signal separation along the phase dimension in phase-rotation technique. When a phase shift, $\mathrm{Exp}(i\ \omega_o\ t)$, is applied to the time-domain signal, $\mathrm{Exp}(i\ \omega\ t)$, then the frequency domain signal $F(\omega)$ can be shifted to $F(\omega-\omega_o)$ upon Fourier transformation.

It is worth noting that as the phase increment, $\Delta\phi$, decreases, signals from different CTPs become less dispersed in the phase dimension, which makes the process of signal separation

more difficult and increases the chance of signal contamination. However, if $\Delta\phi$ is too large then dispersion becomes too high so that peaks from some CTPs will fall off the top and bottom limits of phase dimension, without folding back into the 2D matrix. It is important to observe signals from all CTPs in a 2D phase-rotation map to be able to separate desired signal from undesired ones and to tailor the design of the pulse sequence to minimise undesired signal. Minimising undesired signal is useful in phase-cycling based acquisition protocols, since if undesired signal is weak, then imperfect signal subtraction artefacts are generally weak. An optimum value for $\Delta\phi$ can be selected by calculating the maximum phase change (mpc) from the phase equations of existing signals as a function of $\Delta\phi$ (Table 1) and making sure that 'nrow $\Delta\phi$ /360' evaluates to a whole number, where 'nrow' is the number of increments in the phase dimension. If 'nrow $\Delta\phi$ /360' is not a whole number, then signal will be partitioned between different rows, instead of one row for each type of signal. Thus, $\Delta\phi$ can have any value described by:

$\Delta\phi$ = 360 wnum/nrow, where wnum = 1,2,3,4, IntegerPart $(\frac{\text{nrow}}{2\,\text{mpc}})$ where IntegerPart gives the integer part of $\frac{\text{nrow}}{2\,\text{mpc}}$, with an upper limit of $\Delta\phi = \frac{180}{\text{mpc}}$.

The nature of a phase-rotation experiment is cyclic, that is, the phases of the three RF pulses in say, a PRESS sequence phase-rotation experiment, are simply repeated every 16 increments in a 22.5°-increment-size experiment. Thus, the spectrum obtained with phases set to 22.5° is equivalent to the spectrum obtained with the phases set to (360° + 22.5°) and (720° + 22.5°) and so on. This is not the case for 2D spectroscopic correlation experiments [18, 19] were a time delay is incremented continuously and no two spectra acquired at different time delays are the same. One might envisage, then, to acquire only the first 16 increments in a phase-rotation experiments and fill up the remaining 112 increments, in a 128-increment experiment, with the first 16 increments. This approach will save time, but is flawed due to the fact that noise averaging and signal averaging will both be coherent during the 2DFT and as a result, there will be no overall improvement in the signal to noise ratio (SNR) of the final desired row.

2. EXPERIMENTAL IMPLEMENTATION OF PHASE-ROTATION SCHEMES ON MR SCANNERS

At the time of writing, phase-rotation schemes are not implemented by manufacturers of MR scanners, since the software was not written to accommodate 2D spectroscopic acquisition and processing. The interested reader will need to manually implement aspects of the protocol to get the phase-rotation experiment working properly.

First, the 1D pulse sequence must be modified so that the phase of particular RF pulses is incremented during the experiment. Free induction decays (FID) must be written to disk individually without averaging as is the case with phase-cycling based methods. At the end of the experiment, the total number of raw FIDs must be concatenated to form one 2D raw data matrix. The concatenation can either be undertaken by modifying the processing software on the scanner, or offline. Bruker software Xwinnmr [20] and MestReC [21] both have built in

protocols to do this concatenation. The raw 2D data is then processed (phase-sensitive mode), and the row of interest is extracted, inverse Fourier-transformed, zero-padded (filled) to double its size, and then Fourier transformed with the appropriate processing parameters. The user must avoid setting $\Delta\phi$ to a value where the desired row is located on row number nrow/2, since signal that is independent of phases of RF pulses will fall on this row, and this might reduce SNR.

3. PHASE-ROTATION VERSUS PHASE-CYCLING

The advantage of the phase-rotation method is that the imperfections due to incomplete signal subtraction are avoided and pure signal can be located at a particular row in the two-dimensional experiment. Artefacts arising from sudden subject movement, a serious problem in in-vivo studies using phase-cycling schemes, can be easily eliminated in phase-rotation schemes due to the unique phase value of the motion-related signal. All effects of signal variation (sudden, periodic, or slow types) are eliminated in phase-rotation technique due to the phase dependence of these signal variations [5].

Phantom studies show that peaks are more symmetrical in phase-rotation than in phase-cycling methods. Resolution is also improved in phase-rotation methods. Phase-rotation based single quantum (STEAM and PRESS) spectra have comparable SNR to phase-cycling ones, but DQF phase-rotation SNR was found to be higher than phase-cycling SNR by about 10-20 %.

4. EXPERIMENTAL

Data were collected on a standard Magnetom 3T Trio system (Siemens AG, Erlangen, Germany), using a circularly polarized (CP) head coil (Siemens AG, Erlangen, Germany) to transmit and receive. A spherical GE brain MRS phantom MRS-HD (GE Medical Systems, Milwaukee, WI) containing the standard brain metabolites (N-acetyl-L-aspartic acid (NAA, 12.5 mM), creatine hydrate (Cr, 10 mM), choline chloride (Ch, 3 mM), myo-inositol (mI, 7.5 mM), L-glutamic acid (Glu, 12.5 mM), DL-lactic acid (Lac, 5 mM), sodium azide (0.1%), potassium phosphate monobasic (KH2PO4, 50 mM), and sodium hydroxide (NaOH, 56 mM) containing 1 ml/l Gd-DPTA (Magnevist)) [22] was used. Water suppression was performed before the pulse sequence by using a WET scheme [23]. Processing was done in Matlab [24] and MestReC [21] programs.

The method was tested on apparently healthy volunteers. This study was approved by the local institutional ethics committee and written informed consent was obtained from participants.

5. STEAM AND PRESS SPECTROSCOPY USING PHASE-ROTATION

STEAM spectroscopy [13, 25] and PRESS spectroscopy [26] sequences were previously implemented in phase-rotation mode by Knight-Scott et al. [4, 27] and Hennig et al. [5], respectively. In PRESS phase-rotation experiment, Hennig et al. [5] was able to reduce TE to 20 ms. This was considered to be quit short in 1992, and was achieved by reducing the duration of spoilers to 2 ms on either side of the 180^{o} RF refocussing pulses with the same

amplitude as the slice-refocussing gradient. Phase increments values were $\Delta\phi1 = -\Delta\phi2 = \Delta\phi3 = 22.5^{o}$. Thus, in a 128-increment experiment, PRESS signal was located on row 24, after 2DFT was applied.

A PRESS phase-rotation spectrum of the brain MRS phantom, acquired without spoilers, is shown in Fig. 1. Five types of signals were obtained and are assigned in Fig. 1. Note that only one of them is considered a "proper" signal. Notice that there was no need to eliminate or cancel undesired signal, but instead it was possible to keep them away from the proper signal on row 24. Phase-cycling will never work if all spoilers are omitted, and the final spectrum in this case will be equivalent to the co-addition of all signals (a-e) in Fig. 1.

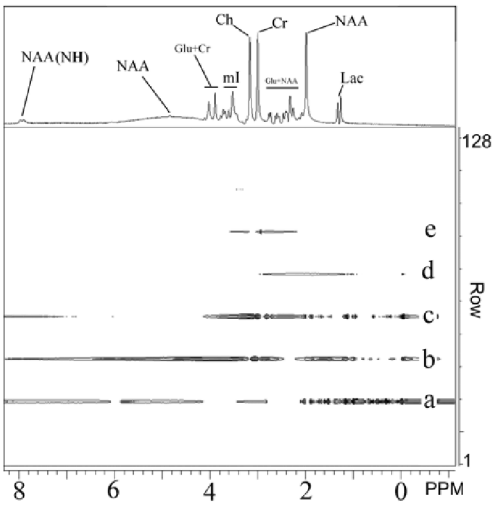

FIGURE 1. PRESS (90^{o} SP1 180^{o} SP1 SP2 180^{o} SP2 Acquire, SP1 and SP2 are spoilers) phase-rotation 2D map of a brain phantom acquired with $\Delta\phi1 = -\Delta\phi2 = \Delta\phi3 = 22.5^{o}$, all spoilers were set to zero, number of averages per increment =1, Number of increments = 128, TR = 2s, bandwidth = 2000 Hz, total experimental time= 4 minutes, water suppression [23] was inserted before the PRESS sequence. Assignment of rows is as follows: a: PRESS signal, b: Echo 23, c: FID 1 + FID 3 + Echo 13, d: FID 2, and e: Echo 12. 1D spectrum on top is a PRESS spectrum (row 24, a). Turning SP1 and SP2 on will eliminate all signals except signal a.

Phase-rotation based STEAM spectroscopy [4, 27] was only implemented some thirteen years after Hennig's original paper [5]. The aim here again was to reduce TE further. A TE of 6 ms was achieved by implementing phase-rotation based acquisition and by shifting all spoilers and slice-refocusing gradients into the 2nd TE/2 delay. This helped also in the spoiling of the relatively large and undesired signal of FID 3. An illustration of STEAM phase-rotation experiment on a phantom is shown in Fig. 2.

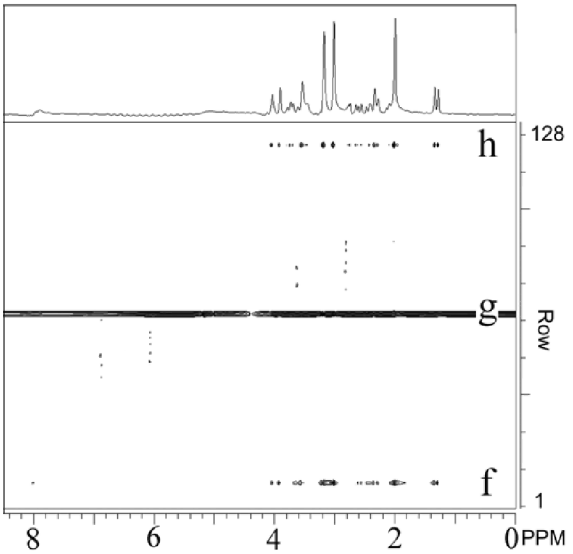

FIGURE 2. STEAM (90° SP1 90° SP2 90° SP1 Acquire, SP1 and SP2 are spoilers) phase-rotation 2D map of phantom acquired with $\Delta\phi1 = 157.5°$, $\Delta\phi2 = \Delta\phi3 = 0°$, all spoilers were set to zero, number of averages per increment =1, Number of increments = 128, TR = 2s, bandwidth = 2000 Hz, total experimental time= 4 minutes, water suppression [23] was inserted before the STEAM sequence. Assignment of rows is as follows: f: FID 1 + STEAM P +PRESS + DQF 3 +DQF 4, g: FID 3 +FID 2 + Echo 23, h: STEAM N + Echo 12 + Echo 13 + DQF 1 + DQF 2. 1D spectrum on top is STEAM spectrum (row 120, h). Turning SP1 and SP2 on will eliminate all signals except signal h. Spectral assignment is the same as in Fig. 1.

The use of a 157.5° phase-step for the 1st RF pulse in STEAM sequence while leaving the phase of all other pulses constant [4] does not seem to be the best design of a STEAM phase-rotation sequence. Whilst such parameters will separate FID 3 from the desired STEAM N signal, but the phase change experienced by STEAM N will be the same as that experienced by Echo12, Echo13, DQF1 and DQF2, which partly defies the purpose of the phase-rotation technique. Even if these unwanted signals do not contain large amounts of signal, they will add noise to the desired row, which will decrease the overall S/N ratio. A better phase-rotation setup is one with $\Delta\phi1 = 22.5°$, $\Delta\phi2 = 67.5°$, $\Delta\phi3 = 45°$, where STEAM N signal can be detected solely on row 32 in a 128 increment phase-rotation experiment. Thus, STEAM N signal can be detected without any signal or noise contamination.

6. DUAL-PRESS

An additional implementation of phase-rotation acquisition is using Dual-PRESS whereby two spectra, instead of one, are acquired in the same experiment. Usually, short and long echo times (TE) localised spectra are acquired from a tissues or organs to show rapidly and slowly relaxing metabolites. In single echo based methods, the echo is acquired until it decays completely. In Dual-PRESS, the short TE is acquired for a shorter time, and then the

remaining signal is refocussed using a refocussing radio frequency (RF) pulse, and another echo-with a longer TE- is collected. Thus, Dual-PRESS effectively saves 50% of the acquisition time, by collecting the two echoes in a single experiment. An additional advantage of the proposed sequence is that T2 can be reasonably estimated for the observed metabolites. Ideally, a multiple point fitting curve at many values of TE is preferred for an optimal T_2 measurement.

7. THEORY

In this experiment two echoes are acquired in the phase-rotation mode. The proposed pulse sequence is shown in Fig. 3.

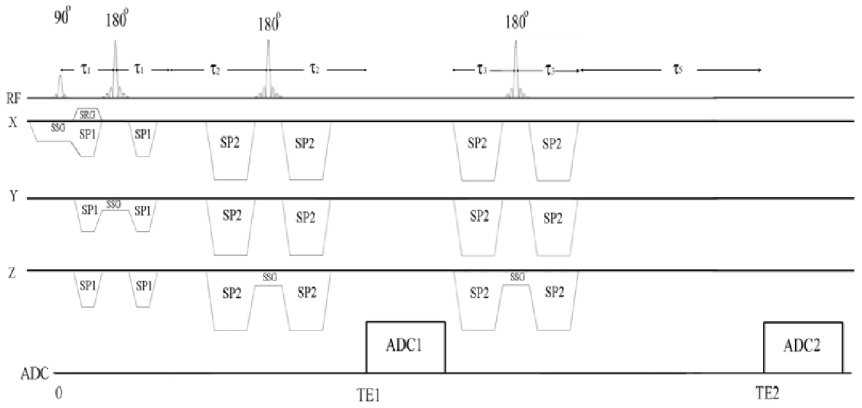

FIGURE 3. A dual-PRESS pulse sequence showing TE1=2*τ1+2*τ2, TE2=TE1+2*τ3+2*ADC1, spoiler gradient pulses SP1 and SP2, slice selection gradients (SSG), slice refocussing gradients (SRG), ADC1 and ADC2. SRG and SP1 are applied as one gradient, and are shown separately for clarity. Note that τ5 must be equal to ADC1 if a phase-sensitive echo2 is desired, otherwise τ5 can be set to zero to collect maximum signal.

Phase-rotation approach was used to collect data using the Dual-PRESS protocol. The data was not averaged in time domain, but was arrayed into a 2D matrix. 2D-FT was implemented and the desired signal detected on a specific row in the 2D map. The position of the row depends on phase-increments size, and number of increments [6].

Note that each 180° RF pulse is surrounded by a pair of spoiler gradients pulses along the three logical axes. The three spoiler pulse pairs have different amplitudes and durations to eliminate any stimulated echo signal. The spoiler gradients of last 180° RF pulse must be made strong enough to spoil any free induction decay (FID) which is usually produced by a tissue that does not experience a perfect refocusing pulse. This FID can be detected as a weak signal on row 48, if the present phase-increments are used and 128 phase-increments are acquired and if spoilers of last 180° RF are not strong enough. Replacing the last refocusing pulse by a hard 180° RF pulse will produce a second echo, but will also produce a large unwanted FID from inside and outside the voxel/slice. The terminal slice-selective 180° RF

was applied in the transverse plane to reduce any spurious signal associated with sagittal or coronal orientations [28].

The coherence transfer pathway (CTP) [15] for Echo1 and Echo2 are (0, −1,+1,−1) and (0, +1,−1,+1,−1), respectively, assuming quadrature detection. From the CTP of each coherence, the phase equations of Echo1 and Echo2 as a function of RF phases can be calculated:

Echo1: $2\,\phi3 - 2\,\phi2 + \phi1$

Echo2: $2\,\phi4 - 2\,\phi3 + 2\,\phi2 - \phi1$

where $\phi1, \phi2, \phi3, \phi4$ are the phases of the first, second, third and fourth RF pulses, respectively.

The phases of receivers during acquisition of Echo1 and Echo2 signals were kept constant whereas phases of first, second, third and fourth RF pulses where incremented by 11.25°, 33.75°, 78.75° and 45.0°, respectively from one row to another. Thus, in a 128 increment experiment, Echo1 will be detected on the row 28 after applying two-dimensional (2D) Fourier transform (FT) for the 128 concatenated Echo1 raw data files. Similarly, Echo2 will be observed on row 68 after 2DFT is applied to the concatenated 128 Echo2 raw data files. Post-processing details are as described previously [6]. The proposed combination of phase-increments described above is not unique, but was chosen because it keeps the desired signal on a separate row and distinct from any unwanted signal in the final 2D map.

There are many different coherences that can be produced by the proposed combination of four RF pulses [29]. The suggested values of phase-increments ensure that no two coherences occur on the same row after 2D Fourier transform. This ensures the purity of Echo1 and Echo2 signals.

A phase-cycling analogue of the proposed pulse sequence was also implemented, but the quality of the phase-rotated spectrum was superior. Due to imperfect addition/subtraction of unwanted signal, especially in-vivo, some residual spectral feature were observed in the phase-cycled spectrum [4-6, 27].

It is worth noting that Echo1 is fully refocussed due to the balance of time delays and gradient momentums between RF pulses, which means that it can be processed in a phase-sensitive mode. To maximize the amplitude of the heavily relaxed second echo, data acquisition was started immediately after the last spoiler gradient pulse after the terminal 180° RF pulse, i.e. a full echo is acquired. This explains why the second echo was processed in magnitude mode. Acquiring the second echo in phase-sensitive mode can be done if a delay equal to the duration of the first echo is inserted before the second echo. This, however, will reduce the signal amplitude of the second echo due to heavy T_2* weighting. In case of long T_2 species, Echo2 can be phased during post-processing even if full echo signal was acquired by shifting the time-domain data to the left by a duration equal to Echo1.

8. PHANTOM STUDIES

Echo1 and Echo2 were acquired from the brain phantom, using the proposed pulse sequence in phase-rotation mode. 128 phase-increments were acquired, concatenated and doubly Fourier Transformed. Rows corresponding to Echo1 and Echo2 were extracted, inverse-Fourier transformed, zero-filled to 4096 points, and re-Fourier transformed. Phantom Results are shown in Fig. 4. Echo2 was acquired in phase-sensitive mode due to the relatively long T2 values of the metabolites present in the phantom.

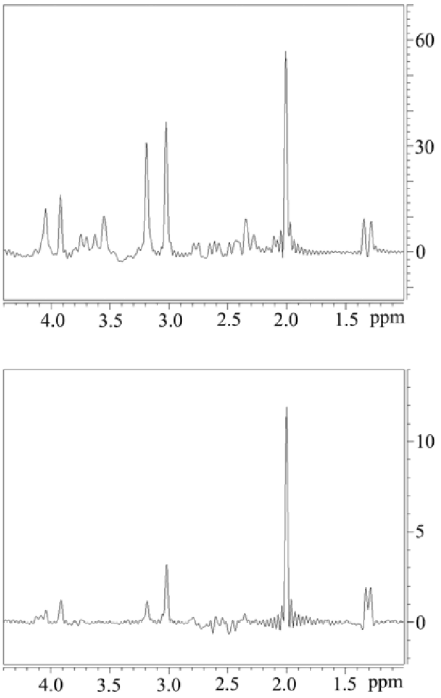

FIGURE 4. 3T MR spectra from a phantom using Echo1 and Echo2 of Dual-PRESS localised single voxel spectrum processed in Mestrec. Acquisition parameters for Echo1 (top) are: TE=30 ms, acquired vector size=512 points, zero-filling to 2048 points, acquisition duration=256 ms, spectral width= 2000 Hz, number of phase-increments=128, voxel size=30x30x30 mm^3. Echo1 was Fourier transformed in phase-sensitive mode after an exponential (line broadening 0.3 Hz) window functions was applied. Acquisition parameters for Echo2 (bottom) are: TE=550 ms, acquired vector size=512 points, zero-filling to 2048 points, acquisition duration=256 ms, spectral width= 2000 Hz, number of phase-increments=128. Echo2 was Fourier transformed in the phase-sensitive mode after an exponential (line broadening 0.3 Hz) window function was applied. WET water suppression scheme [23] was applied prior to the Dual-PRESS sequence. Further removal of water was achieved by convolution method during post-processing. The two spectra are drawn to scale. See text for other details. Spectral assignment is the same as in Fig. 1.

9. HEALTHY VOLUNTEER

An in-vivo Dual-PRESS experiment was undertaken on the brain of an apparently healthy 23 year old and resultant data shown in Fig. 5 and Fig. 6. For comparison, a single voxel, single echo PRESS (traditional) spectrum was acquired from the same region of interest as shown in Fig. 7.

Also, in-vivo T_2 values for Ch, Cr and NAA were measured from a dual-echo experiment, and were found to be 217, 147 and 214 ms, respectively.

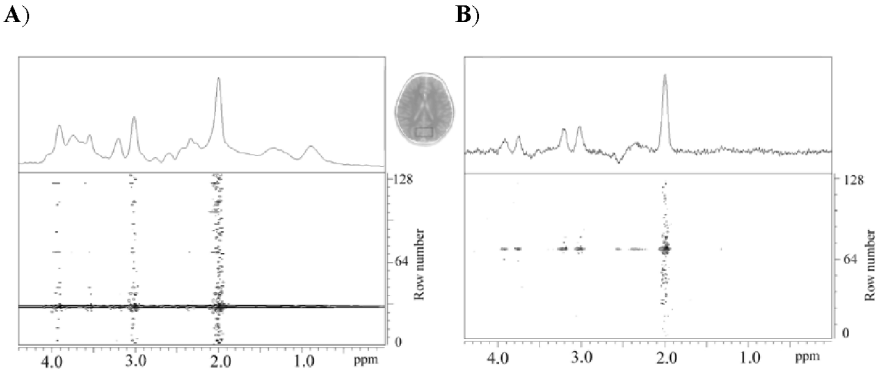

FIGURE 5. 3T in-vivo spectra of Echo1 and Echo2 recorded using the Dual-PRESS in a healthy volunteer and processed in Mestrec. Acquisition parameters for Echo1 (**A**) are: TE=30ms, acquired vector size=256 points, zero-filling to 4096 points, acquisition duration=128 ms, spectral width= 2000 Hz, number of phase-increments=128, voxel size=40x20x30 mm^3. Echo1 was Fourier transformed in the phase-sensitive mode after an exponential (line broadening 0.3 Hz) window functions was applied. The 1D shown on top of 2D is row 28. Acquisition parameters for Echo2 (**B**) are: TE=294ms, acquired vector size=1024 points, zero-filling to 4096 points, acquisition duration=930 ms, spectral width= 1100 Hz, number of phase-increments=128. Echo2 was Fourier transformed in the phase-sensitive mode after an exponential (line broadening of 0.3 Hz) window functions was applied. The 1D shown on top of 2D is row 68. WET water suppression scheme [23] was applied before the Dual-PRESS sequence. Further removal of water was achieved by the convolution method during post-processing. Spectral assignment is the similar to Fig. 1.

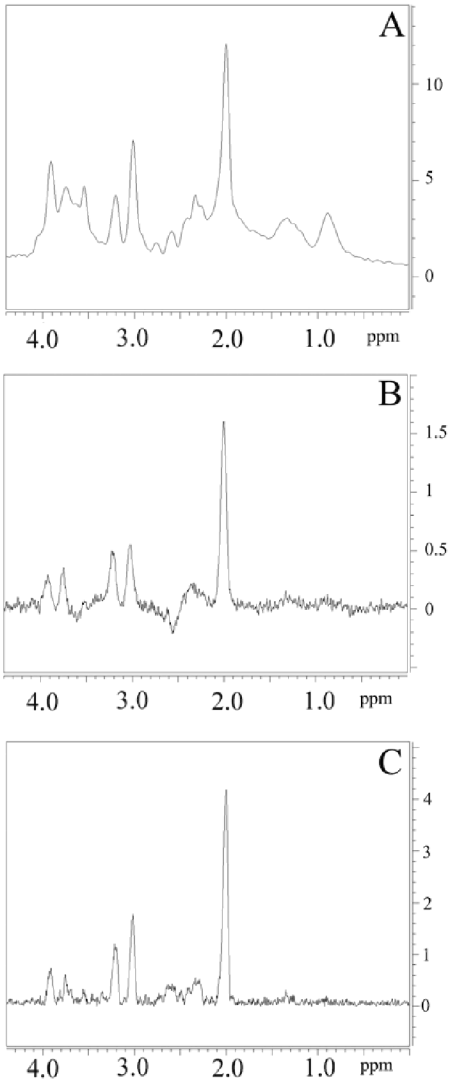

FIGURE 6. 3T in-vivo spectra of Echo1 and Echo2 of Dual-PRESS localised single voxel spectra acquired from a healthy volunteer and processed in Mestrec. Spectra **A** and **B** are the same spectra shown in Fig. 5. Acquisition parameters for spectrum **C**, which is the "full" second echo of a phase-rotation experiment, are: TE=166 ms, acquired vector size=1024 points, zero-filling to 4096 points, acquisition duration=930 ms, spectral width= 1100 Hz, number of phase-increments=128. Echo2 was Fourier transformed in magnitude mode. WET water suppression scheme [23] was applied before Dual-PRESS sequence. Further removal of water was achieved by convolution method during post-processing. The spectra are drawn to scale. Spectral assignment is the similar to Fig. 1.

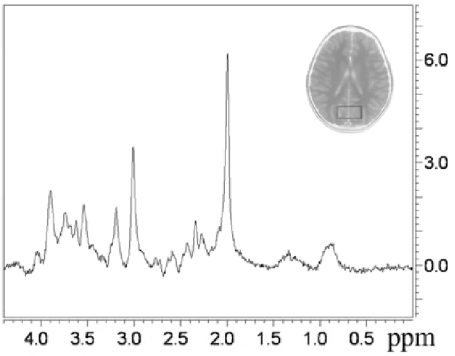

FIGURE 7. 3T in-vivo PRESS localised and water suppressed MR spectrum acquired from a healthy volunteer and processed in Mestrec. Acquisition parameters are: TE=30ms, acquired vector size=1024 points, acquisition time=512 ms, spectral width= 2000 Hz, number of averages=32, voxel size=40x20x30 mm^3. WET water suppression scheme [23] was applied before PRESS sequence. Further removal of water was achieved by convolution method during post-processing. Raw data was zero filled to 2048 points and multiplied by an exponential window function (line broadening factor = 0.3 Hz) before Fourier transform. Spectral assignment is the similar to Fig. 1.

10. DISCUSSION

The short and long TE spectra shown in Fig. 6 have different types of spectral information, but they were both acquired using the same experimental protocol. While the short TE spectrum shows both long and short T2 species, macromolecules and lipids, the long TE spectrum show resonances of Ch, Cr and NAA only which are expected to have long T_2. Strongly J-modulated species (e.g. Glu, glutamine (Gln), γ-aminobutyric acid (GABA) and mI) are heavily attenuated in the long TE spectrum, and are too weak to be detected in the second echo.

The validity of metabolite quantitation by peak fitting in a truncated time-domain signal, was proven by comparing the quantitation results of a truncated time-domain signal with those obtained from a fully acquired one. Differences between the two quantitations were within negligible experimental error.

The implementation of phase-rotation for both echoes ensures that detected signal actually arise from the interrogated voxel. Extraneous signal has a different phase and if survived spoilers, would show up on different row numbers in the final 2D map.

The application of Pade transform [30, 31] to Echo1 due to its relatively short acquisition duration, might bring about some spectral improvement, especially in resolution. However, the traditional Fourier transform results were comparable to those obtained from fully acquired spectral data, and no attempt was done to implement Pade transform.

In addition to the short and long TE spectra obtained in a single experiment, the proposed pulse sequence provides a quick and efficient method to measure T_2 relaxation times of

spectral singlets. Singlet peaks of Ch, Cr and NAA methyl groups at 3.18, 3.03 and 2.00 ppm [32] are most suited to illustrate the T_2 evaluation feature due to minimal spectral interference and absence of J coupling. Measuring T_2 from a series of spectra acquired at different TE is well documented [16, 29, 33]. Thus, T_2 can be obtained from the slope of the straight line obtained when TE is plotted against –ln(S), where S is the peak area [16, 29].

Using in-vivo data from fully refocussed first and second echoes (A and B in Fig. 6), the T_2 values obtained for Ch, Cr and NAA were 217, 147 and 214 ms, respectively. These results match very well with T_2 values reported in the literature [34, 35].

Note that when the second echo is non-refocussed, it cannot be used for T_2 measurements, due to the effect of magnetic inhomogeneities present during the first half of the second echo, and the absence of chemical shift refocussing. However, a more intense, non-refocussed second echo can still be used for non-quantitative purposes.

11. CONCLUSIONS

The phase-rotated Dual-PRESS method allows two localized single voxel short and long TE spectra to be acquired in a single experiment. This method saves 50% of the experimental time and provides T_2 values for different metabolites in water suppressed 1H MR spectroscopy.

ACKNOWLEDGMENTS

This work was supported by a grant from the Australian Research Council (DP0663987).

REFERENCES

1. Kingsley PB. Product Operators, Coherence Pathways, and Cycling Part I: Product Operators, Spin-Spin Coupling, and Coherence Pathways. Concepts in Magnetic Resonance 1995;7:29-47.
2. Kingsley PB. Product Operators, Coherence Pathways, and Phase Cycling. Part III: Phase Cycling. Concepts in Magnetic Resonance 1995;7:167-192.
3. Levitt MH. Spin Dynamics: Basics of Nuclear Magnetic Resonance. Chichester: Wiley & Sons; 2001.
4. Knight-Scott J, Shanbhag D, Dunham S. A phase rotation scheme for achieving very short echo times with localized stimulated echo spectroscopy. Magn Reson Imaging 2005;23:871-876.
5. Hennig J. The application of phase rotation for localized in vivo proton spectroscopy with short echo times. J Magn Reson 1992;96:40-49.
6. Ramadan S. Phase-Rotation in In-vivo Localised Spectroscopy. Concepts in Magnetic Resonance 2007;30:147-153.
7. Frahm J, Michaelis T, Merboldt K, Bruhn H, Gyngell M, Hanicke W. Improvments in localised Proton NMR spectroascopy of Human Brain. Water suppression, short echo times, and 1 ml resolution. J Magn Reson 1990;90:464-473.
8. Mlynarik V, Gruber S, Starcuk Z, Starcuk Z, Jr., Moser E. Very Short Echo Time Proton MR Spectroscopy of Human Brain With a Standard Transmit/Receive Surface Coil. Magn Reson Med 2000;44:964-967.

9. Seeger U, Klose U, Seitz D, Nagele T, Lutz O, Grodd W. Proton spectroscopy of human brain with very short echo time using gradient amplitudes. Magn Reson Imaging 1998;16:55-62.
10. Tkac I, Andersen P, Adriany G, Merkle H, Ugurbil K, Gruetter R. In Vivo 1H NMR Spectroscopy of the Human Brain at 7 T. Magn Reson Med 2001;46:451-456.
11. Tkac I, Starcuk Z, Choi IY, Gruetter R. In Vivo 1H NMR Spectroscopy of Rat Brain at 1 ms Echo Time. Magn Reson Med 1999;41:649-656.
12. Zhong K, Ernst T. Localized In Vivo Human 1H MRS at Very Short Echo Times. Magn Reson Med 2004;52:898-901.
13. Moonen CT, von Kienlin M, Van Zijl CPM, et al. Comparison of Single-Shot Localisation Methods (STEAM and PRESS) for In Vivo Proton NMR Spectroscopy. NMR Biomed 1989;2:201-208.
14. Diehl P, Fluck E, Gunther H, Kosfeld R, Seeling J, editors. In Vivo Magnetic Resonance Spectroscopy II : Localization and Spectral Editing. Volume 27. Berlin, Heidelberg: Springer Verlag; 1992.
15. Ernst RR, Bodenhausen G, Wokaun A. Principles of nuclear magnetic resonance in one and two dimensions. New York : Oxford University Press: Clarendon Press; 1987.
16. Bernstein MA, King KF, Zhou XJ. Handbook of MRI Pulse Sequences. Amsterdam; Boston: Elsevier Academic Press; 2004.
17. De Graaf RA, Rothman DL. In Vivo Detection and Quantification of Scalar Coupled 1H NMR Resonances. Conc Magn Reson 2001;13:32-76.
18. Claridge TDW. High-resolution NMR techniques in organic chemistry: Amsterdam ; Oxford : Pergamon; 1999.
19. Derome AE. Modern NMR techniques for chemistry research. Oxford ; New York: Pergamon Press; 1987.
20. XWINNMR. Bruker BioSpin. Version 3.5. Karlsruhe, Germany; 2006.
21. MestReC. www.mestrec.com. V 4.9.9.1; 1996-2006.
22. Schirmer T, Auer DP. On the reliability of quantitative clinical magnetic resonance spectroscopy of the human brain. NMR Biomed 2000;13:28-36.
23. Ogg RJ, Kingsley PB, Taylor JS. WET, a T1- and B1- insensitive Water-Suppression Method for in vivo Localized 1H NMR Spectroscopy. J Magn Reson Ser B 1994;104:1-10.
24. MathWorks. MATLAB. 7.0.1.24704 (R14); 1984-2004.
25. Frahm J, Merboldt K, Hanicke W. Localized Proton Spectroscopy Using Stimulated Echoes. J Magn Reson 1987;72:502-508.
26. Bottomley PA. Spatial localisation in NMR spectroscopy in vivo. Ann N Y Acad Sci 1987;508:333-348.
27. Knight-Scott J, Dunham SA, Shanbhag DD. Phase Rotation with Asymmetric RF Pulses in Localized Stimulated Echo Spectroscopy (PRAISES) : A 2.5-ms TE Sequence for Clinical Spectroscopy. Proceedings of the Internation Society of Magnetic Resonance in Medicine 2006;14:3052.
28. Ernst T, Chang L. Elimination of Artifacts in Short Echo Time 'H MR Spectroscopy of the Frontal Lobe. Magnetic Resonance in Medicine 1996;36:462-468.
29. Haacke EM, Brown RW, Thompson MR, Venkatesan R. Magnetic resonance imaging: physical principles and sequence design. New York; Chichester: J. Wiley & Sons; 1999. 494 p.

30. Belkic D, Belkic K. In vivo magnetic resonance spectroscopy by the fast Pade transform. Physics in Medicne and Biology 2006;51:1049-1075.
31. Williamson DC, Hawesa H, Thacker NA, Williams SR. Robust Quantification of Short Echo Time 1H Magnetic Resonance Spectra using the Pade´ Approximant. Magnetic Resonance in Medicine 2006;55:762-771.
32. Govindaraju V, Young K, Maudsley AA. Proton NMR chemical shifts and coupling constants for brain metabolites. NMR Biomed 2000;13:129-153.
33. Kreis R, Ernst T, Ross BD. Absolute Quantititation of Water and Metabolites in the Human Brain. II Metabolite Concentration. J Magn Reson Ser B 1993;102:9-19.
34. Barker PB, Hearshen DO, Boska MD. Single-Voxel Proton MRS of the Human Brain at 1.5T and 3.0T. Magnetic Resonance in Medicine 2001;45:765-769.
35. Mlynarik V, Gruber S, Moser E. Proton T1 and T2 relaxation times of human brain metabolites at 3 Tesla. NMR in Biomedicine 2001;14:325-331.
36. Zhu JM, Smith ICP. Stimulated Anti-Echo Selection in Spatially Localized NMR Spectroscopy. Journal of Magnetic Resonance 1999;136:1-5.